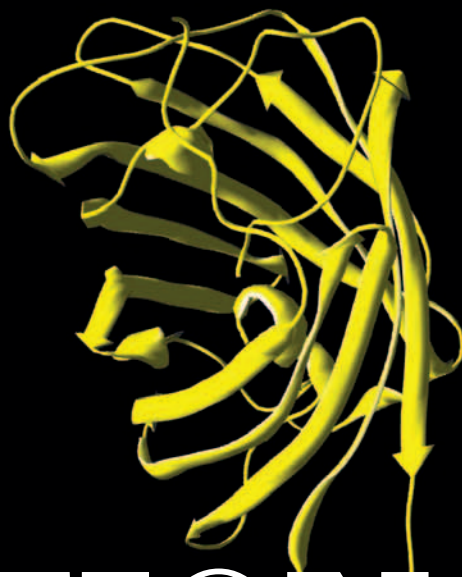


June
2009
No. 35

CONFOCAL APPLICATION LETTER

A 3D ribbon diagram of a protein structure, colored blue, positioned on the left side of the cover, partially overlapping the title.

reSOLUTION

FRET with FLIM

Quantitative *In-vivo* Biochemistry

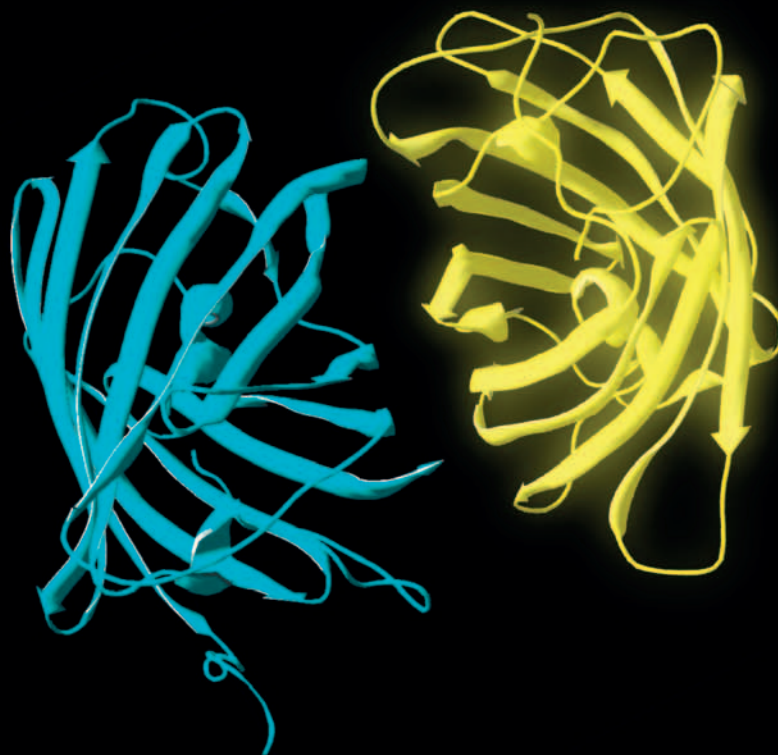


Fig. 1 Emission spectrum of donor (here ECFP, blue line) must overlap with excitation spectrum of acceptor (here EYFP, yellow line). This requirement means that both molecules in the FRET pair possess compatible energy levels.

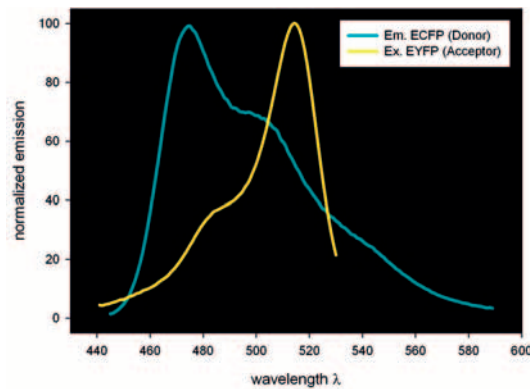


Fig. 2 The donor molecule (D) is separated by a distance r from the acceptor molecule (A).

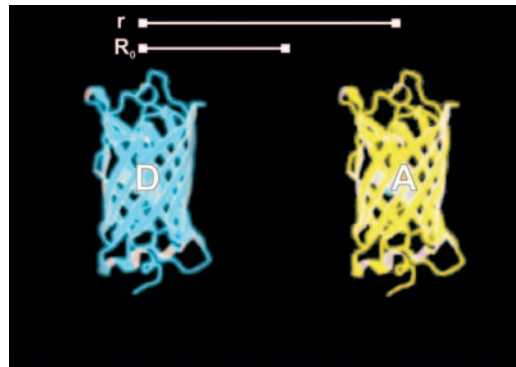


Fig. 3 At a distance r much larger than a threshold value R_0 , also known as the Förster radius, there is no energy transfer.

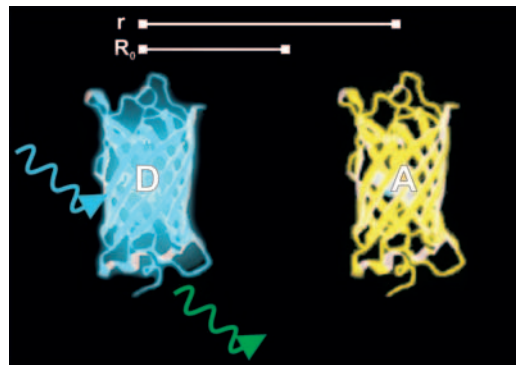
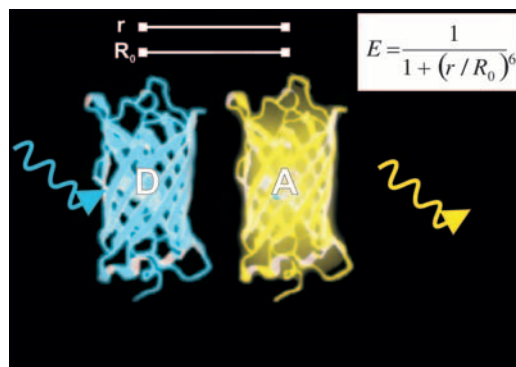


Fig. 4 If the molecules are in close contact energy from the exciting photon (blue arrow) is transferred non-radiatively to the acceptor. In turn, the latter emits a photon (yellow arrow). The efficiency of this process (E) is strongly distance dependent with r^{-6} .



FRET – The Principle

Fluorescence resonance energy transfer (FRET) describes the non-radiative transfer of energy stored in an excited fluorescent molecule (the donor) to a non-excited different fluorescent molecule (the acceptor) in its vicinity. Three conditions must be fulfilled for FRET to take place:

- Overlap of donor emission spectrum with acceptor excitation spectrum (Fig. 1)
- Molecules must be in close proximity on a nanometer (10^{-9} m) scale (Fig. 2–4)
- Molecules must have the appropriate relative orientation

The Impact

Due to its strong distance dependence with r^{-6} (Fig. 4) FRET occurs on a spatial scale which is highly relevant for biochemical reactions, such as protein-protein or protein-DNA interactions. FRET can probe molecular interactions by a sensitive fluorescence read-out. This allows researchers to study molecular interactions both *in vitro* and *in vivo*. By linking two interaction partners of interest with suitable fluorescent labels it is possible to analyze bi-molecular interactions. Alternatively, FRET allows the construction of biological probes reporting concentrations of second messengers or ion strength by means of an intra-molecular FRET due to strong conformational change.

Not surprisingly, FRET has developed into a widely used tool in cell biology, biophysics and biomedical imaging.

The Methodology

There are different techniques to detect FRET in the context of microscopy. Commonly known are techniques based on fluorescence intensity of either the donor (acceptor-photobleaching, FRET AB) or the acceptor (sensitized emission, FRET SE). These methods are described in Leica application letters No. 28 and No. 20, respectively.

Intensity-based FRET can be readily applied using standard confocal microscopes. However, it also has some drawbacks. FRET AB cannot be applied in time series experiments and is susceptible to reversible photobleaching or

photoconversion of the donor molecules. FRET SE, on the other hand, suffers from spectral cross-talk inherent to all FRET pairs and requires careful calibration measurements as well as linear unmixing of resulting images. This application letter introduces a different approach to measuring FRET which is based on fluorescence lifetime imaging microscopy (FLIM).

Fluorescence Lifetime

The process of fluorescence is often understood in terms of energy transitions from the electronic ground state (S_0) to its excited state (S_1) in a molecule (Fig. 5, left). Such transitions can be elicited by incident light with the appropriate energy (i.e. frequency or wavelength). The absorbed energy is stored by the fluorescent molecule for a short time before it can be emitted as fluorescence. The time a molecule spends in its excited state is known as the fluorescence lifetime. It is typically in the order of nano-seconds (10^{-9} s) for many organic dyes and fluorescent proteins.

Fluorescence lifetime and FRET

An alternative process to relax from the excited state is, for example, FRET. By FRET excitation energy is non-radiatively transferred to an acceptor molecule. The acceptor in turn can relax by fluorescence (Fig. 5, right). Since donor fluorescence and energy transfer are competing processes the rate depleting the excited state increases in the presence of FRET. One might say, the longer the donor molecules spend in the excited state the more likely it is that FRET occurs. Only those photons from donor molecules which relax by fluorescence are observed. Energy transferred to acceptor molecules is not detected due to the longer wavelength of acceptor fluorescence. Therefore, FRET shortens the donor lifetime (Fig. 6).

Fluorescence lifetime imaging (FLIM)

The Leica TCS SMD series measures fluorescence lifetimes in the time domain using pulsed lasers and single photon counting detectors. The lifetime is determined by building up a histogram of detected fluorescence events. This reveals a single or multi-exponential fluorescence decay. Numerical curve fitting renders the fluorescence lifetime and the amplitude (i.e., number of detected photons).

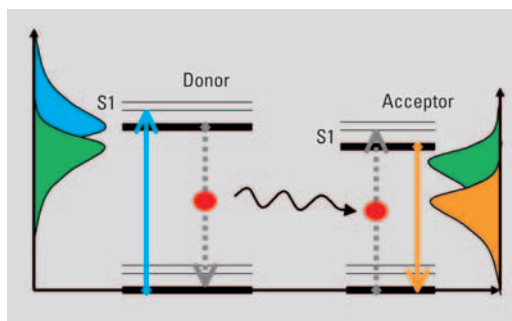


Fig. 5 Energy transitions in a FRET pair. Light energy matching a transition in the donor molecule is absorbed (blue arrow). The excited donor can relax either by fluorescence (gray dotted arrow, left) or by resonance energy transfer to the acceptor molecule (black arrow).

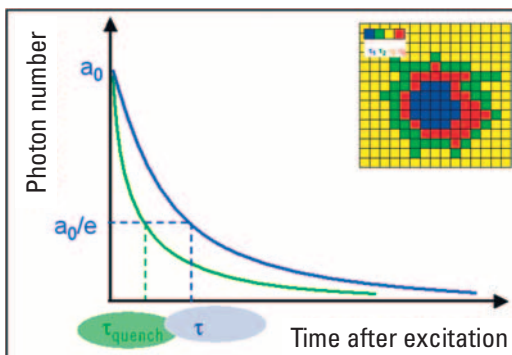


Fig. 6 Plotting the fluorescence photon number over elapsed time after excitation. The initial number of emitted photons after the excitation pulse, a_0 , decays exponentially. The fluorescence takes time to decay to a_0/e (~ 37%) is the fluorescence lifetime. Lifetime τ shifts to shorter times due to FRET (τ_{quench}). Another read-out from the lifetime decay is the amplitude a_0 . Measuring the lifetime at each position in a scanning system yields a spatial map of fluorescence lifetimes (see inset).

FLIM-FRET

Since FRET decreases the donor lifetime one can quantify the extent to which FRET occurs, provided the donor lifetime without FRET is known. This donor lifetime τ serves as an absolute reference against which the FRET sample is analyzed. Therefore, FLIM-FRET is internally calibrated – a property alleviating many of the shortcomings of intensity-based FRET measurements. Since its fluorescence lifetime is an inherent property of a dye it is widely invariant to otherwise detrimental effects such as photobleaching, image shading, varying concentrations or expression levels.

The major limitation using intensity based FRET measurement is the underlying assumption that all observable donor molecules undergo FRET. This is usually not the case. This varying “unbound” fraction of donor molecules introduces considerable uncertainty to the measured FRET efficiency, making comparisons between experiments impossible. FLIM-FRET overcomes this disadvantage.

Fig. 7 RBKB78 cells transfected with a CFP donor only (A) and CFP-YFP fusion (B). The detection band was set between 445 – 495 nm using spectral FLIM detectors. The colored region has been used for analysis. Colors represent intensity modulated fluorescence lifetimes. Courtesy of Prof. Gregory Harms, University of Würzburg, Germany. We acknowledge experimental support by Dr. Benedikt Krämer (Picoquant, Berlin), Jan-Hendrik Spille and Wiebke Buck.

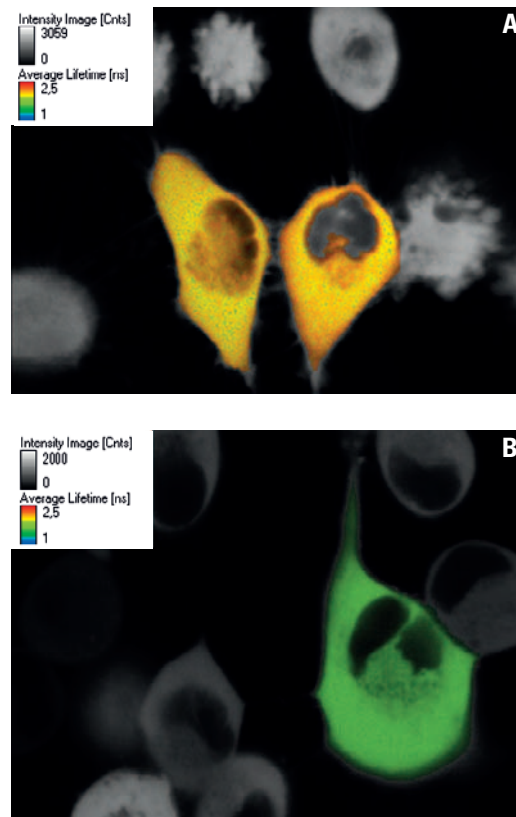
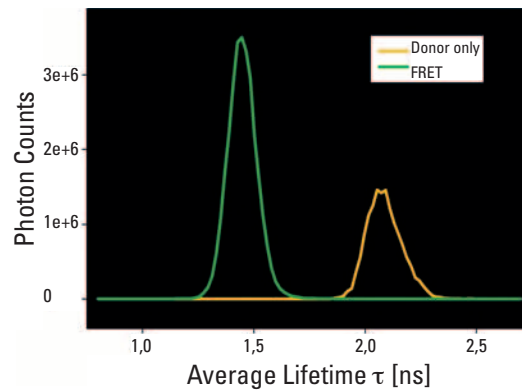


Fig. 8 Fluorescence lifetime distribution of donor only (yellow) and FRET (green) samples using average lifetimes. There is a clear shift of 0.7 ns towards shorter lifetimes in the FRET sample.



Recording FLIM images using live cells

As mentioned previously, the FRET efficiency is computed from the ratio of the fretting donor lifetime τ_{quench} over the non-fretting lifetime τ as:

$$E = 1 - \frac{\tau_{\text{quench}}}{\tau} = 1 - \frac{\tau_{\text{donor,FRET}}}{\tau_{\text{donor,noFRET}}}$$

To this end τ must be known from a measurement using a sample which contains the donor only. It is important to exclude any emission from the acceptor. Using external detectors one must

use a band pass filter. Internal detectors can be adjusted to record only donor emission. The same settings must be used for both the donor-only measurement as well as the measurement using the FRET sample.

CFP-YFP FRET in live cells

In this work we use cultured RBKB78 cells transiently transfected with a FRET construct consisting of a CFP-YFP fusion protein (Fig. 7). The two FPs are connected by a short linker of two amino acids [1]. Such a donor-acceptor fusion can also serve as a good positive control for FRET in a real-world scenario. The “donor only” sample consists of the same cells transfected with CFP only (Fig. 7 A). As a first approximation the average lifetime was computed in fast FLIM mode, for both, the donor only and the FRET sample (Fig. 7 B). The lifetime distribution histograms indicate that the average lifetime t of the donor is 2.1 ns (Fig. 8). The donor lifetime of the FRET construct is 1.4 ns. One obtains a FRET efficiency $E = 1 - (1.4/2.1) = 33 \%$.

Ratios of FRET vs. no-FRET

It is known for CFP to have at least two lifetime components in its own right [2, 3]. Also, it is *a priori* not known whether all molecules under study undergo FRET. In order to do justice to this complexity one needs to have information on more than the average lifetime. We can perform a two-component fit which will give us two lifetimes and two amplitudes. The latter allow us to estimate the relative proportions of one lifetime over the other. In particular, using the amplitudes we can estimate the relative proportions of the fraction exhibiting FRET (bound fraction) and the fraction not exhibiting FRET (unbound fraction). FPs with a weak second fraction, such as EGFP or Sapphire are ideal for this type of analysis.

A more detailed description of each step in the process will be elaborated in the following.

Protocol: Measuring the donor lifetime

The measurement is completely controlled via LAS AF. The necessary steps are explained here:

Three steps to FLIM

An application wizard dedicated to FLIM guides the user along the necessary steps to perform a FLIM experiment. There are three main steps in this workflow (Figs. 9, 10):

- **Setup Imaging:** Find the correct focus, zoom and position in the sample (1), possibly using cw lasers (2) and internal (non-FLIM) (3) detectors. The measurement is started by clicking “Live”, “Capture Image” and “Start” (4). Optionally step 1 can be skipped. Once the desired region has been selected, one can proceed to the next step.
- **Setup FLIM:** One can choose whether to use internal or external detectors (5). Depending on this choice the multifunction port (MFP) (6), the external port (X1-port) (7), analyzer filter wheel (8) and detectors are automatically configured (9). The user only chooses the appropriate laser wavelength (10), laser intensity (external) and number of detectors. One can produce a FLIM preview image by clicking “RunFLIMTest” (11). Estimated average lifetimes are displayed color-coded in the SymPhoTime software and the count rate is fed back to the FLIM wizard (12).
- **Measurement:** Once optimal settings have been found, the last step allows the integration time of a FLIM image to be specified in one of three ways (13). This is done either explicitly as recording time, or as a number of iterations to be integrated or, lastly, as the number of photons in the brightest pixel. In the latter case the integration stops once a user-specified maximum number of photons has been reached. These settings can be combined with complex experiments, such as image stacks in 3D, lambda (wavelength) scans or FLIM time series. The measurement is started by clicking “RunFLIM” (14).

Now that the data has been recorded we can proceed with data processing in SymPhoTime to estimate the donor lifetime.

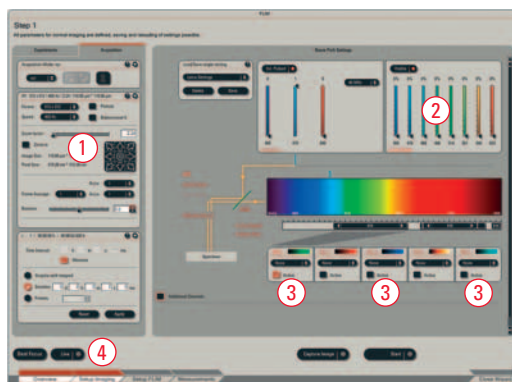


Fig. 9 Step 1 – Setup Imaging. This step allows overview scans or stacks to be performed with non-FLIM detectors. These images can serve as references or could be recorded along with the FLIM images in later steps.

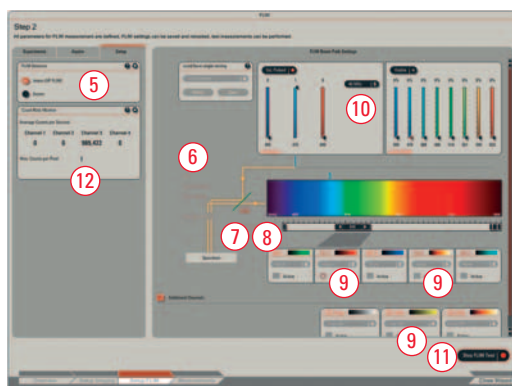


Fig. 10 Step 2 – Setup FLIM. Here one can adjust recording conditions for FLIM. The user can choose from either internal or external detectors and pulsed lasers for excitation, depending on the system configuration. The count rate is displayed and can be adjusted by changing the illumination intensity. Recording conditions, resolution, scan frequency, stacks and time series can be adjusted and tested here. A fast-FLIM preview is available.

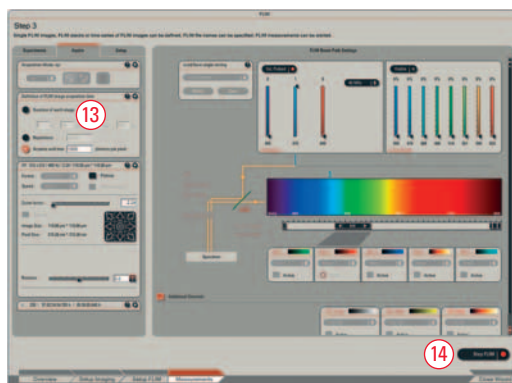


Fig. 11 Step 3 – Measurement. With the settings established in step 2 the data is recorded with a user-defined recording time or photon statistics. An experiment name is defined to facilitate data management across system boundaries.

Fig. 12 Donor only sample. Using ROI tools the cell of interest was selected and the overall average lifetime is displayed in a histogram of all lifetimes in ROI. A false color-scaling was applied ranging from 1.7 ns to 2.8 ns. The intensity image (gray) is overlaid by a lifetime map (color). Data courtesy of Dr. Matthias Weiss, Dr. Jędrzej Szymanski and Nina Malchus, DKFZ, Heidelberg and Bioquant, University of Heidelberg.

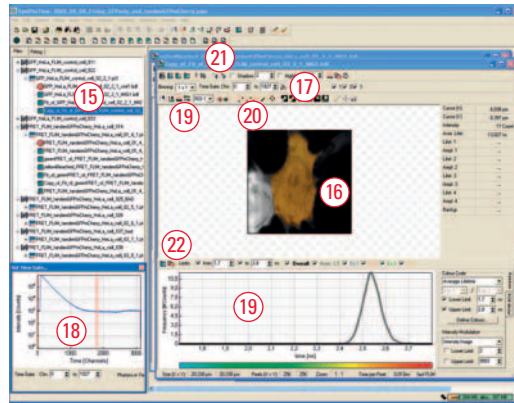


Fig. 13 Fusion of donor and acceptor reveals quenched donor lifetime as displayed in a histogram of average lifetimes.

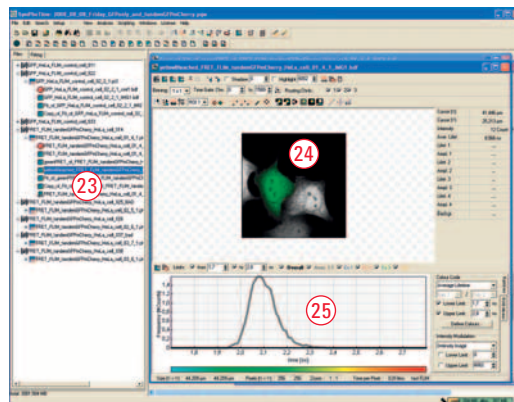
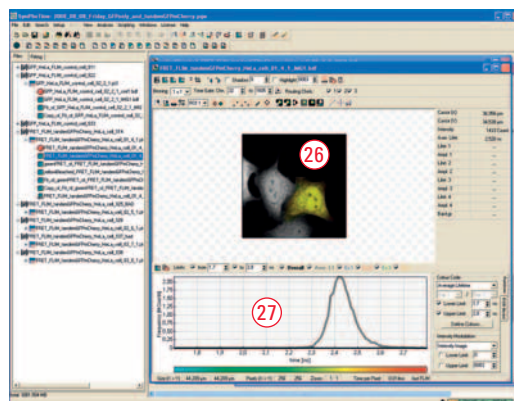


Fig. 14 Photobleaching of acceptor reverts donor lifetime almost to its non-quenched value.



Analysis of FLIM-FRET data – Average lifetimes

The first step in data analysis is to find the appropriate data set and define the desired region. We will use two data sets, one being a donor-only sample consisting of HeLa cells transfected with EGFP. The other, the FRET sample, has been transfected with an EGFP-mCherry fusion construct.

We begin using the donor-only sample. Open the desired data set (15). The appearing window contains a fast-FLIM preview with the average lifetimes (16). We can apply a time gate to crop background photons (17 + 18). Open the lifetime distribution view (19). By default, it uses the entire image. However, we would like to use only the cell in the middle. Activate the magic wand tool (20) and click on this cell in (16). Use the “add” and “subtract” geometry tools together with the magic wand or other ROI tools as needed to work out the geometry of the cell as displayed (20). You may use the digital zoom (21) to enlarge small structures. After ROI selection you can recalculate the lifetime distribution (22) using the highlighted region. Now we can get an estimate for the average lifetime within the selected region assuming its homogeneity: τ_{GFP} is ~ 2.53 ns. Next, we should take a look at the FRET sample. We open the appropriate data set (23). The fast-FLIM image appears (24). For now, we concentrate on the left cell. We perform the steps as described above to select it. The lifetime distribution reveals a shift of the average lifetime to $\tau_{\text{FRET}} \sim 2.08$ ns (25). Using the previously mentioned formula we can compute a FRET efficiency as $E = 1 - (2.08/2.53) = 18\%$.

Controls

In the same preparation a quick control was made to check if the donor lifetime reverts to the donor only situation if the acceptor is abolished (26). This was achieved by photobleaching the mCherry using the 561 nm laser. Using the same strategy as before, we obtain an average lifetime of 2.43 ns (27). We note that this is close to the donor-only lifetime measured during calibration is still somewhat larger. This underlines that for calibration one must always use a sample which has been transfected with a donor-only construct. Even if a cell appears to contain only donor, such as the photobleached one here, there always may be residual traces of acceptor which quench the donor lifetime to lower values. Other important controls could be:

- Transfection with donor and acceptor, which are neither fused to one another nor to any functional protein: Check if presence of acceptor changes donor lifetime. This defines the bottom end of the FRET range for this sample.

- Transfection with a fusion construct of donor and acceptor as presented here can serve as a positive control in a real-world setting. This defines the top end of the FRET range. Together with the previous negative control this yields the dynamic range for FRET for this sample.

Numerical curve fitting of fluorescence decay

So far, we have obtained a good overview of the donor lifetimes in FRET and calibration samples. For a more detailed picture we may now switch to the curve fitting view. Let's start with the GFP sample again. We open the lifetime decay histogram (28). When opening it for the first time the decay histogram is composed of all pixels in the entire image. We create a copy (29) of the previous data set which saves us having to work out the same geometry again. This is done by right-clicking/copy from the context menu or by clicking Ctrl-D. We have to recalculate the histogram from the current ROI by clicking (30). The measured data is plotted in blue. The rising flank (before the maximum) of the histogram is dominated by the response time of the instrument (so-called instrument response function, IRF), while the falling flank contains the useful information on fluorescence lifetimes. We can either perform a tail fit (using some part of the falling flank) or use the complete histogram and perform a reconvolution with the IRF. To do the latter, we use an estimated IRF by selecting (31). A red peak appears. We also have to select the fitting range between the purple cursors (32). We select the entire range by clicking (33). Then we move the cursors (32) to the appropriate positions as shown. We set a few fitting options in the submenu (34). There we select "Use MLE" and un-select any upper or lower limits and press OK.

Model selection

Now that everything is prepared for performing the curve fitting we have to make up our minds as to which model we use. The simplest case is a mono-exponential model. To start with this we set "Exp" to 1 (35) and press "Fit" (36). A black curve appears representing the lifetime decay based on the current fitting model. On the right hand side the optimized parameters are displayed. We obtain an amplitude which is scaled in photons, and a lifetime scaled in nanoseconds (37). The other three parameters serve only for optimizing the fit. We obtain a lifetime around

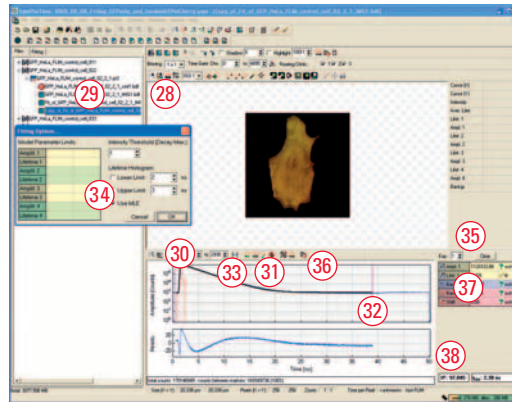


Fig. 15 Single exponential decay (i.e., one lifetime component) and calculated IRF. Large χ^2 and undulating residuals indicate a poor fit.

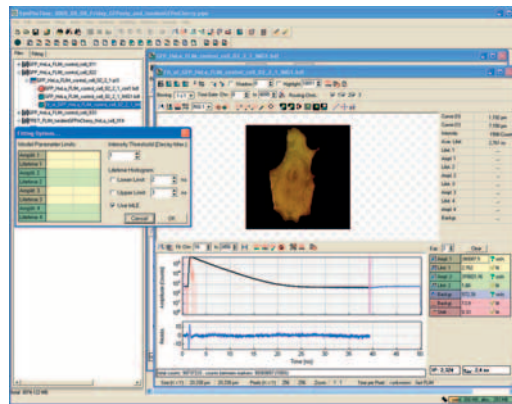


Fig. 16 Extending the model towards two components dramatically improves the quality of the fit. This underlines the bi-exponential nature of the GFP lifetime.

2.4 ns. Let's examine the quality of the fit now: The blue graph below the histogram represents the error residuals, i.e. the difference between data and model. We note that it shows strong undulations. This, together with a large χ^2 value close to 100 (38), suggests that the fit is poor and we need to discard the mono-exponential model.

Bi-exponential model

So, we increase the number of exponentials to 2 (35) and repeat the fit (36). Now we obtain a much more constant residual and a dramatically decreased χ^2 (Fig. 16). Near the rising flank of the IRF (red curve) the residuals are the worst. This may indicate that the estimated IRF does not completely match the real one. This, however, hardly affects the decay. Optionally, a measured IRF can be employed to improve on this. Let's examine the fitting results: we now obtain two amplitudes and two lifetimes.

Fig. 17 Using a three-component curve fit for the analysis of a GFP FRET sample results in a good numerical agreement. We are using all information we have on the donor to reduce the number of fit parameters. The tri-exponential model, however, complicates the interpretation of lifetimes. In the next step we will simplify the model.

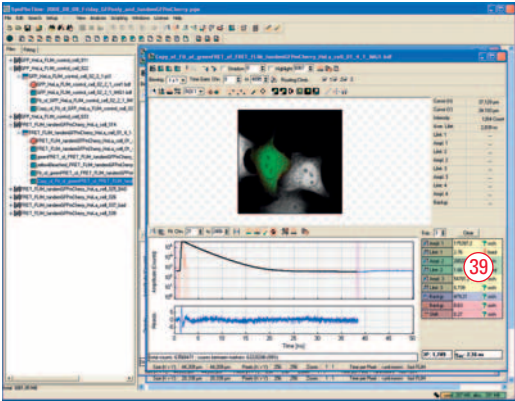


Fig. 18 The average lifetime of the donor only allows us to treat the donor as mono-exponential in the FRET sample. We obtain a similar quality of the fit at the statistical quality level of the data available. This reduction of model complexity allows us to interpret the results in terms of a FRET efficiency in a straightforward way.

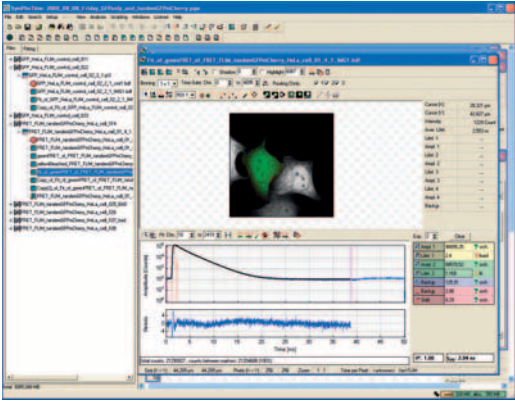
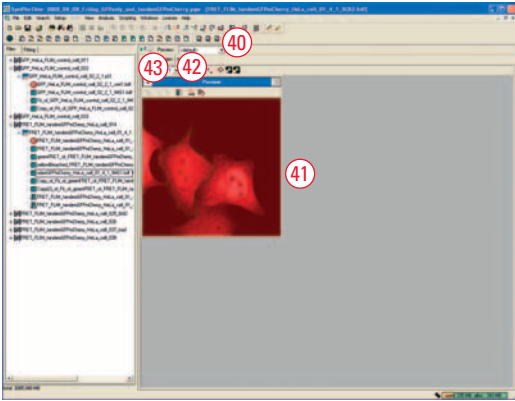


Fig. 19 Computation of FRET efficiencies, Förster radii and bound fraction is greatly facilitated by the use of STUPS-LANG scripts. Here, we select the cell of interest for further analysis.



Interpretation of bi-exponential model parameters

The lifetimes are 2.76 ns and 1.66 ns, respectively. The software also estimates a weighted average lifetime τ_{av} shown at the bottom right (38, right hand side). At 2.4 ns it is equivalent to the estimated single lifetime in the mono-exponential model.

Multi-exponential model fits decay in FRET sample

Seeing that we have a donor which is best

described by a bi-exponential model poses a difficulty now: one or both donor lifetimes can be (partially) quenched by FRET and therefore up to 4 lifetime components would be needed to describe it correctly. The maximum number of exponential terms which can be discriminated in practical terms is, however, three. What happens when using a tri-exponential model? To simplify matters we fix two components to 2.76 and 1.66 ns, respectively, which represents the unquenched (i.e. non-binding) molecules (39). We obtain a good fit and a new quenched fraction with a lifetime of 0.74 ns. This number represents all quenched components.

Model complexity and FRET efficiency

How do we compute a FRET efficiency now? We need to reduce the number of parameters (lifetimes and amplitudes). It is best to use a bi-exponential model. We fix the average lifetime of the donor-only sample, which is 2.4 ns, and let the software fit the remaining two amplitudes and the second lifetime. The agreement between model and data is adequate. From the second lifetime we can now compute the FRET efficiency. We obtain $E = 1 - (1.2/2.4) = 50\%$

Interpretation of FRET results

The real strength of the bi-exponential model is that meaningful amplitudes can be obtained. Using this approach we compute the FRET efficiency of the complete (bound) fraction of FRET molecules. We realize that the FRET efficiency was much lower using average lifetimes only (page 6). There, the efficiency was computed from all molecules, bound and unbound. Depending on the magnitude of the unbound fraction that efficiency will be considerably lower compared to that of the bound fraction. Therefore, $a_1/(a_1+a_2)$ represents the unbound molecule population, conversely, $a_2/(a_1+a_2)$ represents the bound fraction. We obtain 54% unbound and 46 % bound fraction, respectively.

Spatially resolved – Bound fraction and molecular ruler

Thus far we have computed FRET efficiencies and bound fractions averaged for an entire ROI only. Using SymPhoTimes’s scripting capabilities we are able to perform a detailed analysis in a spatially resolved way. The script “FRET/FLIM_FRET_w_Separation” can help us to do this. We

start it by clicking (40). A window appears which allows us to restrict the analysis to a certain area (41) and to apply binning as needed. Binning reduces the spatial resolution while improving the FRET statistics per pixel (42). We proceed through the workflow by clicking (43).

The selected ROI is displayed (44) and the script asks for a user input of the donor only lifetime (45). We employ the same strategy used before and type in the weighted average of the GFP lifetime, in this case 2.4 ns. Optionally, the user can select an intensity threshold for the analysis. We use the default setting and proceed until the computation terminates. The results are displayed concisely inside two tabs, "Images" and "Reports", respectively. The spatial information is contained in the "Images" part. Here, we are presented with a comprehensive set of images highlighting certain aspects of the analysis. Next to the binned intensity and average lifetime images we obtain color-coded maps of the FRET efficiency (46), the bound fraction (47) and the molecular distances in units of the Förster radius. The color coding can be adjusted using a legend tool (48). Essentially, one can draw biochemical conclusions about the binding equilibrium (using the amplitudes) as well as the molecular distances of the bound fraction (using the lifetimes). In this example the maps are relatively homogenous. This is due to our use of a simple donor-acceptor tandem localizing to both cytoplasm and nucleoplasm without any preference.

Dissecting the parameter distribution

All information contained in the images can be summed up in histograms allowing a statistical analysis (49). It is possible to use the ROI tools also post-analysis to get the distribution of any parameter even in a smaller region as needed. We note that, as before, the distribution of FRET efficiencies peaks at about 50 % and the distance of donor and acceptor are about one Förster unit. This is consistent with the definition of the Förster unit. One Förster unit is defined as the distance at which one observes half-maximal FRET efficiency. The workflow presented is a good example for FLIM based FRET measurements, because intensity-based FRET assays usually stop at the step of FRET efficiencies, while binding affinities and radii are not accessible.

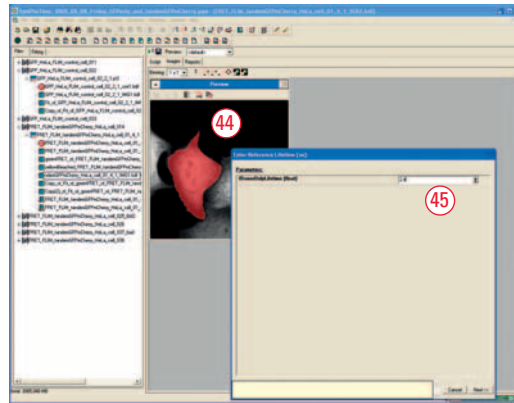


Fig. 20 For computation of FRET efficiencies we need a reference point. We use the average donor only lifetime as one component in the fit model as in Fig. 18.

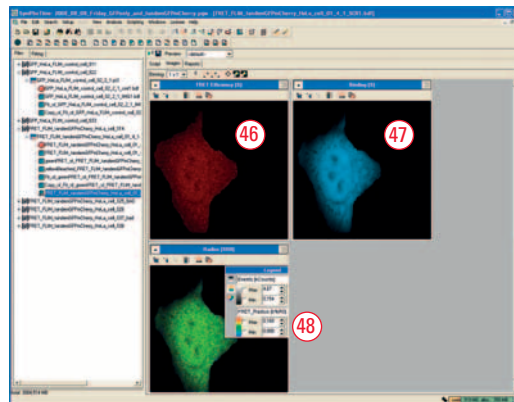


Fig. 21 FRET efficiency, bound fraction and Förster radii are presented in spatially resolved manner. As before, the lifetimes are rather homogeneously distributed throughout, both, cytoplasm and nucleoplasm. We have used a fusion construct which guarantees uniform "binding".

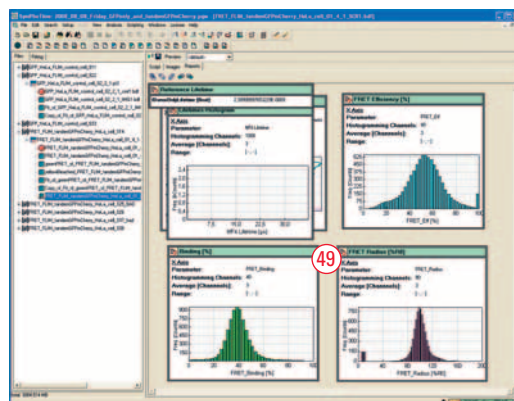


Fig. 22 All parameters are summarized in a report. In this example they are normally distributed. Any inhomogeneities, such as different fluorescent species or different states, might be revealed here.

Fig. 23 Setting up a wavelength scan in LAS AF. The spectral FLIM detector (PMT 4) is used to scan a range from 500 to 620 nm in steps of 30 nm width. In each wavelength band a FLIM image is recorded.

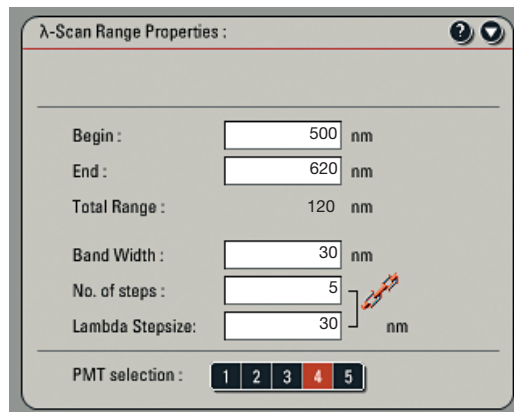


Fig. 24 Donor, FRET sample and controls. A FLIM lambda stack of donor only (upper row), a GFP-mCherry tandem (middle row) and a GFP + mCherry cotransfection (bottom row) were analyzed. The central wavelength of each 30 nm band is given above in nm, colors represent lifetimes according to a LUT as indicated. Live cells courtesy of Dr. Matthias Weiss, DKFZ, Heidelberg.

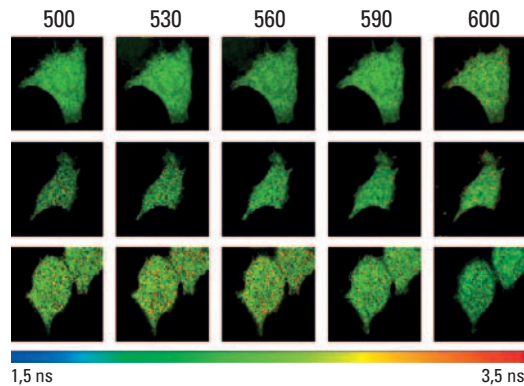
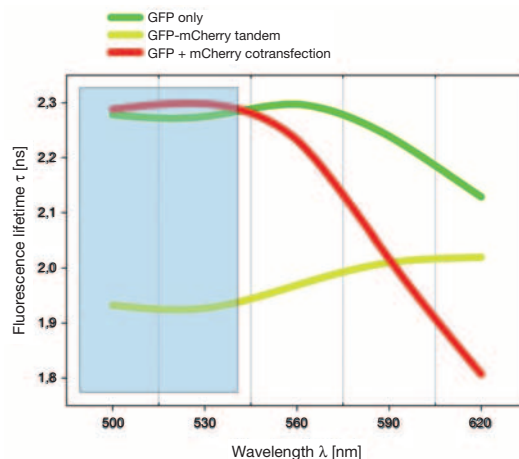


Fig. 25 Fluorescence lifetime vs. wavelength. The lifetime spectra reveal that there is a constant range (gray box) which is suitable for detection of donor emission while at longer detection wavelengths there is contamination by acceptor fluorescence or autofluorescence.



FLIM using spectral detection

As previously explained FLIM measurements are typically standardized using a donor-only sample. The detection window must match the donor emission spectrum and exclude any other fluorescence, such as autofluorescence from the detection. Finding the correct detection range can be time-consuming when band pass filters have to be switched. Here, an approach is presented based on spectrally resolved detection.

The FLIM wizard contains a λ -mode which allows the user to automate recording of a wavelength scan. This option is exclusively available to systems containing internal SP FLIM detectors. We can set the detection range band width, step size, and which detector is going to be used (Fig. 23). In our example we set up five non-overlapping detection bands ranging from 500 ± 15 to 620 ± 15 nm (central wavelength). Again, the sample is a GFP transfected cell culture, as well as cells transfected with a GFP-mCherry tandem (positive control), and with both, GFP and mCherry (negative control). Of all three samples a spectrally resolved FLIM series is recorded. The resulting average lifetimes are plotted over the respective detection wavelength (Fig. 24).

Contamination-free FRET

As evident from Fig. 25, the positive control has the overall lowest lifetime due to donor quenching by FRET. In the lower wavelength range both GFP alone and GFP + mCherry cotransfection display similar lifetimes. However, at large wavelengths the lifetime of both will decrease. This is even more pronounced for the cotransfection. What could cause such a lifetime shift? The answer is found by considering the emission of mCherry. In the 560 nm band (ranging from 545–575 nm) there is already considerable mCherry emission. Therefore, the average lifetime in this range becomes contaminated by a contribution of the acceptor lifetime or by autofluorescence. Even in the donor-only sample there is some evidence of contamination, presumably due to autofluorescence. One should therefore restrict the detection in both calibration and FRET measurements to that range which yields a stable donor signal. In our example this is fulfilled by the two lower detection windows. Failure to restrict the detection range appropriately may lead to grossly biased lifetimes. Moreover, the results may be misinterpreted. This problem only becomes evident if spectral information is taken into account. Spectral FLIM detectors therefore offer more flexibility as well as an optimal detection range for unbiased results.

Informative FRET

We have learned about FRET and how to get a quick qualitative impression of FRET efficiencies. The average lifetimes (fast-FLIM) and histograms

of the lifetime distribution within a given ROI are used. We note that a more detailed analysis using curve fitting with two lifetime components allows the computation of bound vs. unbound fractions. It is important to distinguish between fast-FLIM and multi-exponential curve fitting. The former works by calculating the mean arrival time of fluorescence photons, i.e. the time it takes to decay to half-maximal photon counts. This method is fast enough to allow the display of a real-time FLIM image and it delivers clear images even with low fluorescence intensity or fast time lapse recording. Fast-FLIM serves to give a quick qualitative overview of the spatial lifetime distribution and overall magnitude of lifetimes. However, it can not discriminate background from fluorescence photons yielding potentially biased information. Multi-exponential curve fitting on the other hand allows us to distinguish several lifetimes. It can be performed on a region of interest as demonstrated here or on a per-pixel basis. Next to invaluable biochemical information the curve fitting approach can reveal the existence of a non-fretting fraction of donor molecules. Here, we found only 46% bound fraction for an EGFP-mCherry tandem construct. The non-fretting fraction may, for example, arise due to misfolded fluorescent proteins or truncated translation products. In case of freely diffusing interaction partners a non-fretting fraction can also indicate unbound molecules, which are to be expected from any equilibrium reaction. The assumption that all donor molecules were participating in FRET is therefore typically violated. The FRET efficiency of 18 % computed using the mono-exponential model (all molecules, page 6) versus 50 % estimated from the double exponential model (bound molecules only, page 8) underlines the importance of this differentiation. Any intensity-based FRET measurement ignores this fact and can lead to grossly underestimated FRET efficiencies. Falsely low FRET efficiencies might lead to erroneous interpretation of FRET in terms of the binding affinity. This is always a caveat using intensity-based FRET, which is alleviated by FLIM-FRET.

Choice of dyes

In our examples we used fluorescent proteins only, due to their prominent position in live cell imaging. Generally, for FLIM measurements a label should possess a large molecular brightness, reasonable photostability and ideally its fluorescence should decay mono-exponentially. This latter requirement is often fulfilled by organic dyes typically used in fixed cell labelling. Fluorescent proteins on the other hand tend to display much more complicated photo-physics.

Multiple components reveal FLIM-suitable FPs

None of the FRET donors used here displays a mono-exponential decay. Let's investigate a little bit further: In the equilibrium situation (i.e. in the absence of FRET) one can estimate the relative proportions of each lifetime using the expressions $a_1 \cdot \tau_1 / (a_1 \cdot \tau_1 + a_2 \cdot \tau_2)$ and $a_2 \cdot \tau_2 / (a_1 \cdot \tau_1 + a_2 \cdot \tau_2)$ for the long and the short component,

respectively. Each represents the total number of photons (i.e. area under decay histogram) which is given rise to by the respective lifetime component. This is also known as the intensity-weighted lifetime. If we perform a two-component fit on the donor-only sample we can dissect which lifetime dominates the decay. For ECFP in our sample we found that we need three components to obtain a satisfactory curve fit with 69% of 2.6ns, 25% of 1ns and 6% of 0.3ns. So, for ECFP the relative contribution of each component is different, but we can not ignore at least the second lifetime. Arguably, the third is too short to be determined very precisely, which is the reason why sometimes only two lifetimes are reported for ECFP. For EGFP we find two lifetimes with 67% of 2.8 ns and 33% of 1.7 ns. Note that these values can vary with cell type, cell cycle state and incubation conditions. We conclude that EGFP is much more suitable as a FRET donor using FLIM than ECFP, because of its simpler photophysics. However, we still have to use approximations to reduce model complexity in FLIM-FRET experiments. Generation of suitable FPs is therefore an active field of research and two mono-exponential FP donors have been reported so far, namely Sapphire [4] or mTFP [2]. It is currently not clear which processes lead to the observation of multiple lifetimes, but protein folding or photoconversion might provide possible explanations.

General remark

Due to the general requirement in FLIM to image at relatively low count rates (< 1 MHz) it is recommended to use the 12 bit image format in LAS AF. This will result in much better dynamic resolution of low intensity images. This choice has, however, no influence on the FLIM image or the lifetime, but influences the intensity image recorded in LAS AF only.

References

1. He, L., Olson, D. P., Wu, X., Karpova, T., McNally, J. G., Lipsky, P. E. "A flow cytometric method to detect protein-protein interaction in living cells by directly visualizing donor fluorophore quenching during CFP-YFP fluorescence resonance energy transfer (FRET)" *Cytometry Part A* 55A:71-85 (2003)
2. Al, H., Henderson, J. N., Remington, S. J., Campbell, R. E. "Directed evolution of a monomeric, bright and photostable version of *Clavularia* cyan fluorescent protein: structural characterization and applications in fluorescence imaging" *Biochem. J.* 400:531-540 (2006)
3. Jose, M., Nair, D. K., Reissner, C., Hartig, R., Zuschratter, W. "Photophysics of Clomeleon by FLIM: Discriminating Excited State Reactions along Neuronal Development" *Biophys. J.* 92:2237-2254 (2007)
4. Bayle, V., Nussaume, L., Bhat, R. A. "Combination of Novel Green Fluorescent Protein Mutant TSapphire and DsRed Variant mOrange to Set Up a Versatile in Plant FRET-FLIM Assay" *Plant Physiol.* 148:51-60 (2008)

Acknowledgement

We gratefully acknowledge proofreading by
Dr. Benedikt Krämer, PicoQuant GmbH, Germany

“With the user, for the user”

Leica Microsystems

Leica Microsystems operates globally in four divisions, where we rank with the market leaders.

• Life Science Division

The Leica Microsystems Life Science Division supports the imaging needs of the scientific community with advanced innovation and technical expertise for the visualization, measurement, and analysis of microstructures. Our strong focus on understanding scientific applications puts Leica Microsystems' customers at the leading edge of science.

• Industry Division

The Leica Microsystems Industry Division's focus is to support customers' pursuit of the highest quality end result. Leica Microsystems provide the best and most innovative imaging systems to see, measure, and analyze the microstructures in routine and research industrial applications, materials science, quality control, forensic science investigation, and educational applications.

• Biosystems Division

The Leica Microsystems Biosystems Division brings histopathology labs and researchers the highest-quality, most comprehensive product range. From patient to pathologist, the range includes the ideal product for each histology step and high-productivity workflow solutions for the entire lab. With complete histology systems featuring innovative automation and Novocastra™ reagents, Leica Microsystems creates better patient care through rapid turnaround, diagnostic confidence, and close customer collaboration.

• Surgical Division

The Leica Microsystems Surgical Division's focus is to partner with and support surgeons and their care of patients with the highest-quality, most innovative surgical microscope technology today and into the future.

The statement by Ernst Leitz in 1907, “with the user, for the user,” describes the fruitful collaboration with end users and driving force of innovation at Leica Microsystems. We have developed five brand values to live up to this tradition: Pioneering, High-end Quality, Team Spirit, Dedication to Science, and Continuous Improvement. For us, living up to these values means: **Living up to Life.**

Active worldwide

Australia:	North Ryde	Tel. +61 2 8870 3500	Fax +61 2 9878 1055
Austria:	Vienna	Tel. +43 1 486 80 50 0	Fax +43 1 486 80 50 30
Belgium:	Groot Bijgaarden	Tel. +32 2 790 98 50	Fax +32 2 790 98 68
Canada:	Richmond Hill/Ontario	Tel. +1 905 762 2000	Fax +1 905 762 8937
Denmark:	Herlev	Tel. +45 4454 0101	Fax +45 4454 0111
France:	Nanterre Cedex	Tel. +33 811 000 664	Fax +33 1 56 05 23 23
Germany:	Wetzlar	Tel. +49 64 41 29 40 00	Fax +49 64 41 29 41 55
Italy:	Milan	Tel. +39 02 574 861	Fax +39 02 574 03392
Japan:	Tokyo	Tel. +81 3 5421 2800	Fax +81 3 5421 2896
Korea:	Seoul	Tel. +82 2 514 65 43	Fax +82 2 514 65 48
Netherlands:	Rijswijk	Tel. +31 70 4132 100	Fax +31 70 4132 109
People's Rep. of China:	Hong Kong	Tel. +852 2564 6699	Fax +852 2564 4163
Portugal:	Lisbon	Tel. +351 21 388 9112	Fax +351 21 385 4668
Singapore		Tel. +65 6779 7823	Fax +65 6773 0628
Spain:	Barcelona	Tel. +34 93 494 95 30	Fax +34 93 494 95 32
Sweden:	Kista	Tel. +46 8 625 45 45	Fax +46 8 625 45 10
Switzerland:	Heerbrugg	Tel. +41 71 726 34 34	Fax +41 71 726 34 44
United Kingdom:	Milton Keynes	Tel. +44 1908 246 246	Fax +44 1908 609 992
USA:	Bannockburn/Illinois	Tel. +1 847 405 0123	Fax +1 847 405 0164

and representatives in more than 100 countries